

On Contributions of Two-Particle Correlation Functions to the Intermittent Behavior in Heavy-Ion Collisions

Abdelnasser M. Tawfik

FB Physik, Marburg University, D-35032 Marburg, Germany

Abstract

The factorial moments (FM) of the multiplicity distributions in one- and two-dimensions are studied for Pb+Pb collisions at 158 AGeV. Obvious intermittence slopes are observed in the relation between FM, and the partition number M . The Bose–Einstein correlations (BEC) are investigated in the emulsion data sample. The influences of the two-particle correlation functions (TPCF) on the scaling behavior of FM are also investigated. The dependence of TPCF on the invariant relative momentum Q , as well as on the pseudo-rapidity, $\delta\eta$, are calculated. It is found that TPCF fulfill the requirements of the power-law scaling comparable with the scaling rule of FM. The expected TPCF contributions to FM are quantitatively estimated.

Keywords: fluctuations, intermittence, Bose–Einstein correlations, many–particle correlation functions, strip integral correlations, heavy–ion collisions, quark–gluon plasma

Pacs: 25.75.G, 61.43, 12.38.M, 64.60.Q

1 Introduction

The intensity interference between the produced particles is the unique experimental tool to directly probe the space-time evolution of the interacting system. First, it was used in the radio-astronomy (HBT) [1] to estimate the astronomical distances. After that, the principles of HBT are used by G. Goldhaber, S. Goldhaber, W. Lee and A. Pais (GGLP), in order to study the angular distribution of produced particles in $p-\bar{p}$ annihilation [2]. GGLP describes the phenomenon, that the like-sign charged (identical) particles are emitted within space angles smaller than that of unlike-sign charged (non-identical) ones. Evidently, this

appears as a reason of the symmetrical properties of boson wave functions and therefore, the emission probability is very sensitive to the *Bose–Einstein statistics*. GGLP is therefore known as Bose–Einstein correlations (BEC). In this article, we consider the simplest case of two-particle correlation functions (TPCF), namely BEC. It is known that the shape of TPCF enhancement depending on the relative momentum Q can be related to the emission source dimension R [2] and/or to its life time τ [3]. In principle, the interference between identical produced particles occurs and consequently their TPCF get powerful, when certain conditions are satisfactorily fulfilled. The produced particles should be non-coherent and simultaneously emitted, i.e. the following similar to the Heisenberg’s uncertainty relation has to be satisfied. $\Delta p \cdot \Delta r \leq 2\pi\hbar$ [1, 2, 4, 5]. $\Delta p = |p_1 - p_2|$, and $\Delta r = |r_1 - r_2|$ are the relative momentum and distance of the considered particle pair, respectively. In heavy-ion collisions the typical dimension of the emission source is $\Delta r \approx 6$ fm [6]. Then the interference takes place for Δp up to 50 MeV/c [7]. As mentioned above, TPCF can be used to directly measure many important parameters (e.g. dimension, lifetime, expansion velocity of the emission source). These measurements are highly necessary to study the dynamics of strong interactions and also to probe whether the energy density exceeds the critical value to produce the quark-gluon plasma (QGP) [8, 9].

The two-particle interferometry is recently used to study the dynamics of emission source until the final state of particle production [10]. The Fourier transformation of the space-time density distribution of emission source can experimentally be estimated by TPCF. Generally, the intensity interference is not a characteristic phenomenon of bosons alone. It can also be applied for the fermions. Of course, for fermions, the intensity correlations appear due to the decreased likelihood. Furthermore, the two-proton interferometry introduced in [11] is an effective applicable tool at low energy. Since the protons, in contrast to the pions, were present and effectively participating in all phases of the colliding system from the beginning until the *freeze-out*. The suggestion of the particle–antiparticle interferometry [12] is generally based on the discrepancies between the s-channels of the particle–antiparticle, and that of the particle–particle interactions.

Coming to the second topic of this article; the factorial moments (FM) which have found increasing interest among the high energy physicists, since the pioneer works of Bailas and Peschanski during the second half of 1980’s [13]. The concept “intermittence” is evidently used to describe the fluctuations in the density distributions of particle production, i.e. the power law of FM as functions of the successive phase-space partitions $\delta\eta \rightarrow 0$. To get a satisfactory explanation for such power-scaling behavior, many models are proposed. All these theoretical approaches are trying to give an answer to the question: “What are the possible sources of the power-law behavior in the multi-particle production?” [14]. Following is a short list of some of these approaches.

- Self-similar branching processes,
- Conventional short-range correlations,

- Multi-particle cascade at the final state,
- Critical second-order phase transition to QGP.

Besides these dynamical sources, there are some features [15, 16, 17] for the responsibility of TPCF for the enhanced particle fluctuations, especially in small phase-space intervals. Through successive decreasing the relative momentum of two identical particles, an exponential increasing of their TPCF is high probably expected. Here we are trying to ascertain whether the reduction of the phase-space of pseudo-rapidity $\Delta\eta$, which basically are performed to investigate FM, conducts to auxiliary enhancement of TPCF or vice versa. Experimentally, quite strong evidences are registered [17] for the increment of TPCF with successive reduction of relative momentum $Q = |p_1 - p_2|$, as well as with the decreasing of the pseudo-rapidity phase-space $\delta\eta = |\eta_1 - \eta_2|$.

In this paper both subjects and their traces in Pb+Pb collisions at 158 AGeV are researched. For the data acquisition and the experimental setup we refer to [18, 19] and also to the next section. Here it is important to emphasize that by using the nuclear emulsion one has on the one hand angular resolution and local accuracy as good as ~ 1 mrad and $1 \mu\text{m}$, respectively. But on the other hand the identification of produced particles and the estimation of their charges and impulses can not be achieved. This article is organized as follows: Section 2 introduces the experimental setup. Section 3 deals with the basic definitions and formalism of TPCF, FM, and the strip integral correlations. Section 4 is devoted to the experimental results. Finally, the summary and final conclusions are given in Section 5.

2 Experimental Setup

The data used in this paper are retrieved from some of Pb chambers irradiated at CERN-SPS during 1996 for the EMU01 Collaboration. This material is consummately measured and analyzed at Marburg university by using our measuring system MIRACLE Lab [18, 19, 21]. The collisions are recorded with ^{82}Pb beam accelerated to an incident momentum of 158 AGeV/c and directed towards stationary lead foil with thickness $\sim 250 \mu\text{m}$. The lead foil was positioned in the front of seven plastic sheets coated on both sides by the nuclear emulsion FUJIET-7B. The emulsion is acting in these investigations as detector. The emulsion has a constant area ($10 \times 10 \text{ cm}^2$) but different depths. The first two sheets have emulsions with $180 \mu\text{m}$ in depth. The rest are coated by emulsions with thickness $90 \mu\text{m}$.

The exposure process is mainly controlled by counting the heavily ionizing particles by scintillator and discriminator with relatively high threshold settings. The number of beam particles is counted by using an additional counter installed behind the chamber. Scaler and driver electronics (CAEN N145) are also used to build up and to transfer pulses to the SPS “kicker” magnet which immediately removes the beam when the number of particles transcends 3000 per spot. The spot area is about $6 \mu\text{m}^2$ (beam density of $\sim 5 \cdot 10^2$ nuclei/cm 2).

The number of collisions expected per spot is 17 [20]. The scanning efficiency in the emulsion chamber is 0.75 ± 0.05 [20].

A detailed description of the configuration and the arrangement of the emulsion chamber can be taken from [21]. Because of the relatively high transverse momentum of produced particles and fragmentations most of, if not all, these particles are expected to be concentrated within narrow forward cone. Therefore, their tracks can entirely be registered within the forward emulsions coating the other seven plastic sheets. The emulsion sensitivity for singly charged particles with minimum ionization is found to be as good as 30 grains per 100 μm . Depending on the incoming momentum, the polar angle can be calculated. For the used data sample we get polar angle 1.3 mrad. Also, depending on the target foil and on the topology of the microscope's field-of-view used for the image acquisition [19], the measuring system can effectively acquire secondary tracks with space angles θ up to 30° (pseudo-rapidity values $\eta = -\ln \tan(\theta/2) > 1.32$). The singly charged particles are basically expected to be mixed with small contamination of e^-e^+ pairs coming from γ -conversions in the target foil and from Dalitz production. As a reason of the reconstruction algorithm applied in MIRACLE Lab [19] the tracks of these electrons cannot be grabbed. The possible *overestimation* on the observed particles density is $\sim 2\%$ [21]. In this value all the contributions of γ -conversions in lead foil and in emulsion material have been taken into account. The efficiency of MIRACLE Lab is up to 96%. Large part of this 4% discrepancy is obviously coming from the tracks with relatively large space angle. In addition the missing measurements, frequent scattering, unresolved close pairs, and pair production of e^-e^+ represent another source of such discrepancy [18]. Therefore, we could consciously suggest to renounce the discussion of the effects of γ -conversions on FM.

The investigation of FM is performed for Pb+Pb collisions with particle multiplicity > 1200 . From these central events only the particles observed within predefined pseudo-rapidity intervals are taken into account. These $\Delta\eta$ intervals ($3 < \eta < 4$, $3 < \eta < 5$, $2 < \eta < 5$, and $2 < \eta < 6$) are chosen at as well as around the mid-rapidity region of interaction. The calculation of FM is performed by means of Eq. (6). As discussed before TPCF essentially get an exponential increment while decreasing the relative momenta or decreasing the pseudo-rapidity rather than a linear one. As discussed in [17, 22, 23] TPCF are supposed to contribute to the intermittent behavior of FM with considerable values, especially for small relative momenta Q or for small phase-space partition of pseudo-rapidity $\delta\eta$. But as contemplated in Section 1 the identification of secondary particles is highly required foremost to be able to study TPCF in our experimental data. The identification of produced particles by using the nuclear emulsion evidently is not to put into practice [18, 19, 21]. Furthermore, since there was no external magnetic field applied over the emulsion chambers while the exposure process, measuring the particle momenta is not to be implemented too. Although all these difficulties, I have introduced in [14] three different approximated methods to adapt the calculations of TPCF to the data of nuclear emulsion. For this destination the three algorithms are utilized, in order to nearly identify the produced particles and to approximately estimate

their momenta.

3 Definitions and Formalism

3.1 Two-particle correlation functions

By definition [3, 10, 24], the two-particle correlation functions TPCF and their special case, the Bose–Einstein correlations (BEC) are given as

$$C_2(p_1, p_2) = \frac{P_2(p_1, p_2)}{P_1(p_1)P_1(p_2)}, \quad (1)$$

$$C_2(Q^2) = \mathcal{N} \left[1 + \lambda e^{-\frac{Q^2 R^2}{2}} \right]. \quad (2)$$

λ is the chaos parameter which essentially combines all effects responsible for the chaotic phenomena taking place in and affecting the entire dynamics of the emission source. For example long resonance, coherent particle production, detector resolution, contamination between non-pions and/or secondary produced particles, etc. $P_1(p_i)$ is the probability to detect the i -th single particle emitted with momentum p_i . $P_2(p_i, p_j)$ is the probability to simultaneously detect the i -th and j -th two particles emitted with momentum p_i and p_j , respectively. \mathcal{N} is the normalization factor depending only on the so-called “event mixing” (Section 3.3). By means of the covariant one- and two-particle distributions, the quantities $P_1(p_i)$ and $P_2(p_i, p_j)$ can be expressed in dependence on the multiplicity of one-particle $N_1(p_i)$ and two-particles $N_2(p_i, p_j)$, respectively [25]

$$P_1(p_1) = E_1 \frac{d^3 n}{d^3 p_1} \equiv N_1(p_1), \quad (3)$$

$$P_2(p_1, p_2) = E_1 E_2 \frac{d^6 n}{d^3 p_1 d^3 p_2} \equiv N_2(p_1, p_2). \quad (4)$$

Then TPCF read the following expression

$$C_2(p_1, p_2) = \frac{N_2(p_1, p_2)}{N_1(p_1)N_1(p_2)}. \quad (5)$$

The experimental steps to estimate TPCF and afterwards to calculate the parameters \mathcal{N} , λ , R and/or τ can briefly be summarized as follows:

1. Empirical estimation of C_2 by using the particle multiplicity. This estimation is simply the ratio of the correlated to the non-correlated particles as given in Eq. (5).
2. Choosing an analytical expression for C_2 , for instance Gaussian distribution which can be given in dependence on the dimension of emission source R (Eq. (2)) or also on the life time τ . Depending on the modeling of the emission source density distribution we can extend these analytical

expressions for different dimensions to retrieve estimation for other parameters. For the emulsion data I have driven a special expression given in Eq. (16) [14].

3. Now the last step is more or less clear. Fitting the experimental results of C_2 (step #1) with the analytical ones (step #2), to directly get estimation for \mathcal{N} , R , τ , etc.

3.2 Factorial moments and intermittence exponents

If the phase-space for instance the pseudo-rapidity $\Delta\eta$ is split into M bins of equal sizes $\delta\eta = \Delta\eta/M$ and if n_k being the multiplicity in k -th bin, then the “vertical” FM are given as [13]

$$\langle F_q(M) \rangle = \frac{\langle n_k(n_k - 1) \cdots (n_k - q + 1) \rangle}{\langle n_k \rangle^q}, \quad (6)$$

$\langle n_k \rangle$ is the average multiplicity of the k -th bins of all events. The self-similar density fluctuations for the successive partitions leads to the following power-law scaling.

$$\langle F_q(M) \rangle \propto M^{\phi_q}. \quad (7)$$

The parameters ϕ_q which represent the slopes of the relations $\log F_q$ vs. $\log M$ are called “intermittence exponents”. Their relations with the anomalous dimensions [26] are only depending on the orders q

$$d_q = \frac{\phi_q}{q - 1}. \quad (8)$$

Therefore, for multi-fractal processes d_q can simply be given as functions of q alone. $d_q = d_2$ characterizes the mono-fractal processes, i.e. the particle production can be characterized by one *fractal* dimension.

3.3 Strip integral correlations

The integrals of q -particle inclusive rapidity densities $\rho_q(\eta_1, \eta_2, \dots, \eta_q)$ are conditional to FM given in Eq. (6) [27, 28]

$$\langle F_q \rangle = \left\langle \frac{\int_{\delta\eta} d\eta_1 d\eta_2 \cdots d\eta_q \rho_q(\eta_1, \eta_2, \dots, \eta_q)}{\langle n \rangle^q} \right\rangle. \quad (9)$$

For the ideal case that there is no correlation between produced particles $\rho_q(\eta_1, \eta_2, \dots, \eta_q) = \rho_1(\eta_1)\rho_1(\eta_2) \cdots \rho_1(\eta_q)$ and consequently, $\langle F_q \rangle \rightarrow 1$

$$\langle F_q(\delta\eta) \rangle = \frac{\left\langle \int_{\Omega_k} \prod_{i=1}^q d\eta_i \rho_q(\eta_1, \eta_2, \dots, \eta_q) \right\rangle}{\text{NORM}}. \quad (10)$$

NORM = $\langle \int_{\Omega_k} \prod_i^q d\eta_i \rho_1(\eta_1)\rho_1(\eta_2)\cdots\rho_1(\eta_q) \rangle$ is estimated by the so-called “event mixing” [27]. Generally, the estimation of “NORM” plays a very important role with respect to the final estimation of TPCF. In-offensively, one would suggest to replace “NORM” in last equation by the distribution of non-correlated particles. The difficulties to determine both correlated and non-correlated particles in the emulsion data are frequently discussed before. “NORM” is our data sample — non-correlated particle-pairs — is estimated by using the three methods given in [14] (Section 4.2.2). $\langle \int_{\Omega_k} \cdots \rangle$ in Eq. (10) represents the correlated particle-pairs.

Using the strip integral correlations (Eq. (10)) instead of the conventional sum over the bin multiplicity (Eq. (6)) enables us to entirely avoid the large disadvantage known for the second one, namely the artificial *fake* partitions [23]. In addition to these, the strip integral correlations have other *important* advantages to decrease the statistical errors and to increase the correlation size, etc. [27]. To be able to calculate the integral correlation functions in the pseudo-rapidity phase-space $\Delta\eta$ obviously, we would need to extend the strip integration to another domain, individually depending on the pseudo-rapidity variable η

$$\langle C_q(\delta\eta) \rangle = \frac{\left\langle \int_{\Omega_\eta} \prod_{i=1}^q d\eta_i \rho_q(\eta_1, \eta_2, \cdots, \eta_q) \right\rangle}{\text{NORM}}. \quad (11)$$

Besides the extension into η -domain performance the counting of q -tuples¹ in last equation represents the other difficulty. To avoid this, we use the Grassberger–Hentschel–Procaccia integrals [27, 29]. Therefore, the last strip integration for instance for the second order ($q = 2$) reads the following form

$$\langle C_2(\delta\eta) \rangle = \frac{\left\langle 2! \sum_{j_1 < j_2}^n \prod_{k', k''} \mathcal{H}(\delta\eta - |\eta_{j_{k'}} - \eta_{j_{k''}}|) \right\rangle}{\text{NORM}}. \quad (12)$$

n is the total particle multiplicity inside the whole considered interval $\Delta\eta$ and \mathcal{H} is the “Heaviside” unit step function. Analogue to Eq. (12) and by utilizing suitable algorithm to count the strip integral correlations it is possible to deduce

¹The counting algorithm used in this article has the following instructional iterations

- Determining the phase-space $\Delta\eta$ and the partition width $\delta\eta$. Within each phase-space partition ($\delta\eta$), the differences between the pseudo-rapidity values $\eta_{ij} = \eta_i - \eta_j$; $i < j$ are calculated and then compared with the pre-specified width $\delta\eta$ according to the inner product if Eq. (13).
- Counting the q -tuple of $\{\eta_{ij_1}, \eta_{ij_2}, \cdots, \eta_{ij_q}\}$ from each i -th event of the used data sample by using the *Heaviside* unit step function.
- The results of last counting is then multiplied by $q!$ to take into account the number of permutations within each q -tuple.
- Repeating the last steps for all available $\binom{n}{q} - l$ tuples and then calculating the average over the total events.

a general expression for any order $q \geq 2$. This expression can also be given in dependence on the relative pseudo-rapidity $\delta\eta$ (Eq. (12)) or on the relative momentum Q (Eq. (15)). For the direct relation between both variables Q and $\delta\eta$ we refer to Note #c

$$\langle C_q(Q^2) \rangle = \frac{\left\langle q! \sum_{j_1 < j_2 < \dots < j_q} \prod_{k', k''}^{q-1} \mathcal{H}(Q^2 - \delta Q_{j_{k'}, j_{k''}}^2) \right\rangle}{\text{NORM}}, \quad (13)$$

where $\delta Q_{j_{k'}, j_{k''}}^2 = |Q_{j_{k'}} - Q_{j_{k''}}|^2$. The last relation is perspicuously close coincidence with the expression of the factorial moments given in Eq. (6). By means of this relation, we are apparently succeeded to derive an expression to study the contributions of TPCF to the power-law scaling of the conventional FM.

3.4 TPCF as a possible source of intermittence

Once more the conditions of the validity of two-particle interferometry are given in Section 1. Since the breadth of the emission source is limited within the finite source diameter $2R$, then TPCF (BEC) are effective, if the relative momentum fulfill the following relation

$$\Delta p \leq \frac{\pi\hbar}{R}. \quad (14)$$

In addition, from last expression the particle interferometry (non-coherence phenomenon) strongly takes place, if the breadth of the emission sources $R \rightarrow 0$. Of course we still remember the properties of FM which are suggested as an effective signature for the non-statistical fluctuations at the final state of particle production [13] and then as a diagnostic tool to confirm the QGP formation. FM show power-like behavior for the consecutive dividing of the phase-space $\Delta\eta$ into $\delta\eta \rightarrow 0$ sub-intervals. Equation (14) describes almost the same behavior, namely while the momentum difference is successively decreased $\Delta p \rightarrow 0$, an exponential increasing of TPCF is strongly expected. This behavior remains valid, even if the breadth of emission source R has a constant value (fixed source diameter). In case that the dimension of emission source sanctimoniously suffers a successive explosion or shrinking $R \rightarrow 0$ it is obviously expected that TPCF become more stronger. Practically, the *power-like* behavior of two-particle correlation functions C_2 has been investigated [17] with the successive reduction of the momentum difference $\Delta p \equiv Q \rightarrow 0$ as well as with the successive reduction of the pseudo-rapidity interval $\delta\eta \rightarrow 0$. This leads to the following power law which apparently is to be compared with the scaling rule given in Eq. (7).

$$C_q(\Delta Q) \propto (\Delta Q)^{-\phi_q} \quad (15)$$

TPCF are, as their name announces, the correlations between the particle-pairs in a very restricted region ($\Delta r < 6$ fm and $\Delta p < 50$ MeV/c). Therefore, it is not more difficult to explain why they are supposed to contribute to the compulsory correlations between the produced particles? Especially, if the investigation is

being performed within the region defined above, in which TPCF are effective. For all these reasons it is now more or less clear, if we predict that TPCF can be suggested as possible sources of the “intermittent behavior” in heavy-ion collisions [16, 30].

4 Experimental Results

4.1 Results of factorial moments

In all events of the data sample the four pseudo-rapidity intervals $\Delta\eta$ defined in Section 2 are successively split into $M \rightarrow \infty$ sub-intervals (bins) with equal widths $\delta\eta = \Delta\eta/M \rightarrow 0$. In each such bins the particle multiplicity is counted and then the q -order FM are calculated according to Eq. (6). Figure 1 shows $\log F_q$ as functions of $\log M_\eta$ for the orders $q = \{2, 3, 4\}$. The subscript in M_η means that the phase-space partition has been performed in η -dimension only. Obviously, the experimental results can good be fitted as straight lines according to the scaling rule Eq. (7). The slopes represent the so-called *intermittence slopes* ϕ_q . The four pictures show obvious positive linear tendency. Also, it is to realize that the values of $F_q(M_\eta)$ and ϕ_q increase with decreasing the $\Delta\eta$ intervals. The largest values are obtained within the smallest interval $3 < \eta < 4$. There is another remarkable finding that ϕ_q increase with increasing the orders q (review Eq. (6)).

By continuous increasing the partition number M_η , FM exponentially grow (Fig. 2). The reasons for this fast upwards increasing are discussed in details elsewhere [23]. Here the discussion is restricted only on the phenomenological behavior of the increasing of $F_q(M_\eta)$ with increasing the partition number M_η . Naturally, increasing $\Delta\eta$ intervals enables us to divide the one-dimensional phase-space (η) into large partition number M_η . Once again we also notice in this figure that the range of the linear dependence becomes larger with wider $\Delta\eta$ windows (pictures from top to bottom). This linear dependence are studied in the previous figure. In the top most picture, the curvature upwards increasing has *sharp spikes*. Plateau begins to appear with increasing the $\Delta\eta$ intervals. In the largest interval (bottom most picture) we have the largest plateau covering the distance from $M_\eta \approx 200$ to $M_\eta \approx 600$. Beyond this saturated regions $F_q(M_\eta)$ continue their exponential increasing. This time steeper than before. We continued the partition process $\delta\eta \rightarrow 0$ as long as FM increase.

4.2 Results of TPCF

4.2.1 Adapting TPCF in emulsion data

As shortly introduced before it is expected that TPCF contribute to FM with considerable values, especially, if FM are studied within small phase-space intervals where TPCF are expected to be strongly enhanced (Section 1). Therefore, before the announce whether non-statistical fluctuations (e.g. dynamical) are observed as the case in Fig. 1 and 2, one has to study all possible sources which

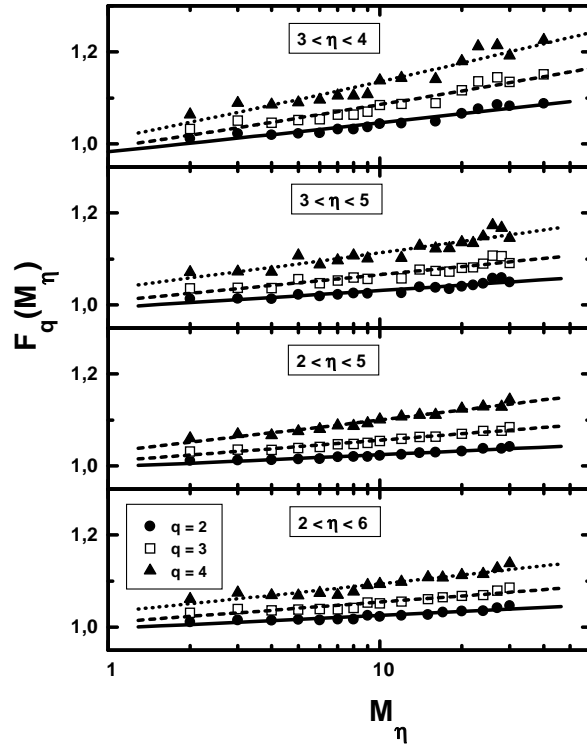


Figure 1: The factorial moments F_q for the orders $q = \{2, 3, 4\}$ are plotted as functions of small partition number M_η . The data used here are Pb+Pb collisions at 158 AGeV with total multiplicity > 1200 . The results can good be fitted as straight lines (Eq. (7)). Their slopes represent the “intermittence exponents” ϕ_q . Although the ordinates are also log scales, their labels are given.

may be responsible for such *abnormal* scaling behavior. After that if the further scaling of FM still establish linear positive tendencies with the partition number, this might be then referred to self-similar branching processes and/or to critical second-order phase transition to QGP [23, 31]. Regard being had to the nature of TPCF alone, one can expect an exponential dependence with the decreasing of the considered phase-space rather than a linear one (review Eq. (2)). As mentioned in Section 1 the identification of produced particles and the estimation of their momenta are highly necessary to be able to study the two-particle interferometry. The two-particle interferometry known as BEC (Section 1) represents the simplest case of TPCF. The identification of produced particle by using nuclear emulsion obviously is not to be put into practice. In [14] three different methods have been introduced and examined to make it possible to estimate TPCF for the emulsion data sample. For these algorithms the

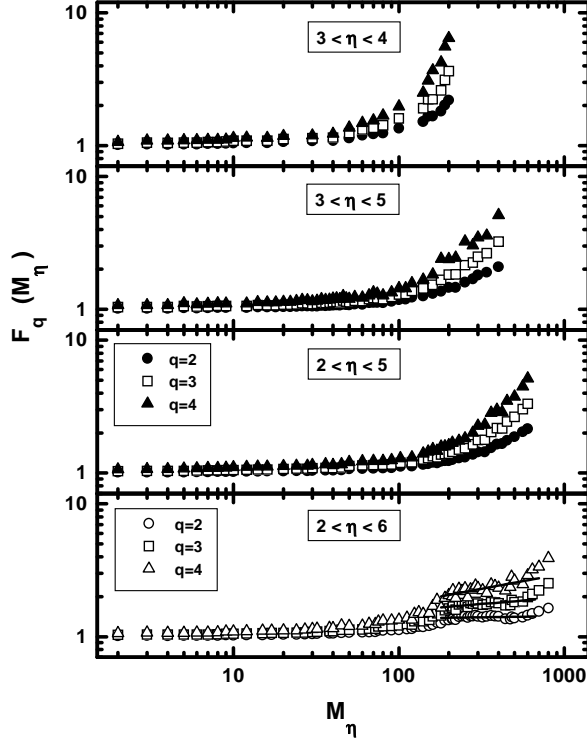


Figure 2: The factorial moments F_q for the orders $q = \{2, 3, 4\}$ are depicted in log-log charts as functions of large partition number M_η . The partition process is repeated as long as FM values increase. An exponential growth of FM is noticed for relatively large M_η . Within the largest $\Delta\eta$ interval, we notice that FM are saturated.

expression given in Eqs (2) and (5) must be modified as follows:

$$C_2^{Em}(Q) = \frac{1}{2} \left[1 + \mathcal{N} \left(1 + \lambda e^{-\frac{Q^2 R^2}{2}} \right) \right]. \quad (16)$$

The prediction of this approximation are compared with the ratios between correlated and non-correlated multiplicity of particle-pairs (Eq. (5)). The superscript in Eq. (16) says that the investigation and consequently, this analytical form are applied for emulsion data sample. The subscript refers to the two-particle correlations BEC. This will be replaced by q , when we will modify Eq. (16) to be compared with FM for the different orders q . The results of Eq. (16) will be depicted in Fig. 3. The fitting parameters \mathcal{N} , R , and λ are compared with the parameters of data samples acquired by other detectors which are in the position of being able to identify the produced particles and to measure their impulses [32].

4.2.2 TPCF as function of Q

Figure 3 shows the dependence of TPCF on the invariant relative momentum Q of all possible particle-pairs of our Pb+Pb data sample observed within the pseudo-rapidity interval $1 < \eta < 10$. For this data set we counted about $\sim 3 \cdot 10^6$ particle-pairs. The averaged *transverse* momentum $\langle p_t \rangle$ is assumed to be constant ~ 350 MeV/c. By using this constant value and the related equations given in [14] it is possible to assign to each particle a stochastically calculated momentum. Then it is possible to calculate the relative momentum Q for each particle pair. The algorithms discussed in [14] are used to count the non-correlated particle-pairs and then to classify their multiplicities according to Q . Counting the correlated particle pairs is now more or less unsophisticated process. In fact the algorithm which randomizes the angular characters of the original events, is preferentially used. Obviously, the randomized particles in this regard represent the background distribution “NORM”. In such a way the normalization factor \mathcal{N} gets an average value fixed around the unity. It is necessary to point out here that no correction for the Coulomb repulsion has been considered, since the amount of Gamov correction factor [33] is $\sim 10\%$ for $Q \approx 1$ MeV/c. With increasing the values of Q Gamov correction factor exponentially decays. As discussed in Section 1 the two-particle interferometry must be taken into account only for $Q \leq 50$ MeV/c. Therefore, the ratios of correlated particle pairs (multiplicity of original events) to the non-correlated ones (multiplicity of background distributions) for $Q > 70$ MeV/c can be fixed to the unity, i.e. for $Q > 70$ MeV/c, we can assume that there is no difference between the multiplicity of correlated and non-correlated particle-pairs.

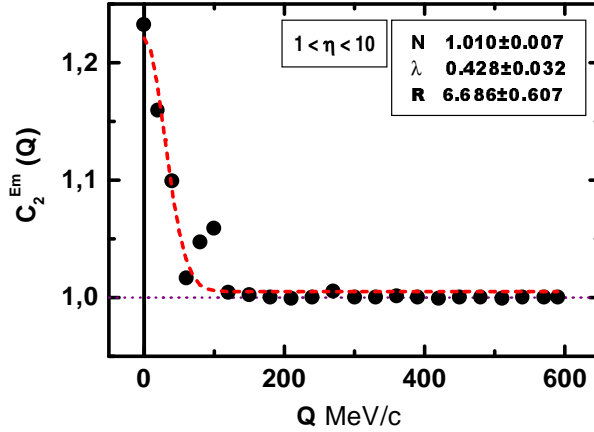


Figure 3: $C_2^{Em}(Q)$ are depicted as functions of the invariant relative momentum Q for the interval $1 < \eta < 10$. The fitting parameters obtained by using the analytical relation Eq. (16) are given at the upper right corner.

The experimental results shown in Fig. 3 are fitted by using Eq. (16). The obtained fitting parameters are $R = 6.686 \pm 0.607$ fm, $\lambda = 0.428 \pm 0.032$, and $\mathcal{N} = 1.010 \pm 0.007$. All these values are comparable with the results obtained from data sample of detectors able to identify the produced particles and to estimate their charges and momenta [32]. For our one-dimensional analysis the resulting parameters are assumed to combine all their corresponding components. Using one-dimensional analytical expression for the correlation functions C as in Eq. (16) which depends only on the invariant relative momentum Q obviously does not enable us to directly investigate the behavior of the other components of R and λ with Q . The breadth of emission source $R = 6.686 \pm 0.607$ fm is on the one hand evidently comparable with the r.m.s. nuclear radius of ^{82}Pb , 7.11 fm on the other hand it shows that the method used here to calculate BEC in emulsion data sample has a very good physical acceptance. The value of the chaos parameter $\lambda < 1$ is an evidence for the partial non-coherent emission source and for the simultaneously emitted particles. As given in Section 3.1 this parameter includes all possible chaotic effects taken place in the emission source. More details about the results of BEC in the emulsion data sample can be obtained from [14].

4.2.3 TPCF as function of η

The conventional TPCF dependence on the invariant relative momentum Q does not enable us to directly² study their contributions to the intermittent behavior observed in the experimental data (Fig. 1 and 2). For this purpose, it is needed to study as evident as possible the direct TPCF dependence on the pseudo-rapidity η or alternatively to investigate their behavior within the region, $Q < 50$ MeV/c. Such a way it will be possible to check whether their behavior can be given by a power law similar to that of FM, i.e. whether TPCF are also intermittent. Section 4.2.4 is devoted to the second suggestion. The behavior for large interval $0.5 < Q < 100$ MeV/c will be studied and compared with the results given in Section 4.1. In this section we study the direct dependence of C_2^{Em} on the pseudo-rapidity phase-space $\delta\eta$.

Figure 4A shows the dependence of C_2^{Em} on $\delta\eta$ for the pseudo-rapidity interval $1 < \eta < 10$. The intervals between the successive iterations of $\delta\eta$'s are constant (0.1). Taking the different statistical acceptances into account we notice that the step-wise successive increasing of $\delta\eta = |\eta_1 - \eta_2|$ leads to slow *linear* decreasing of C_2^{Em} until the value $\delta\eta \approx 2.0$. This value is corresponding to space angles $\theta \approx 15^\circ$, i.e. TPCF of particle-pairs distributed up to $\sim 15^\circ$ are able to

² Since the invariant relative momentum Q on the one hand depends on the squared invariant mass $Q^2 = M_{inv}^2 - (im)^2$, it can be used to study the fluctuations due to cluster resonance decay. On the other hand this relation reads

$$Q^2 = [p_{1t}^2 + p_{2t}^2 + 2p_{1t}^2 p_{2t}^2 \cos(\delta\phi)] - [M_{1t}^2 + M_{2t}^2 + 2M_{1t}^2 M_{2t}^2 \cos(\delta\eta)].$$

This relation implies that for given $\delta\phi = |\phi_1 - \phi_2|$, $Q = |p_1 - p_2|$ can be given in dependence on $\delta\eta = |\eta_1 - \eta_2|$. Such a way TPCF can also be studied in dependence on the phase-space partition of pseudo-rapidity $\delta\eta$.

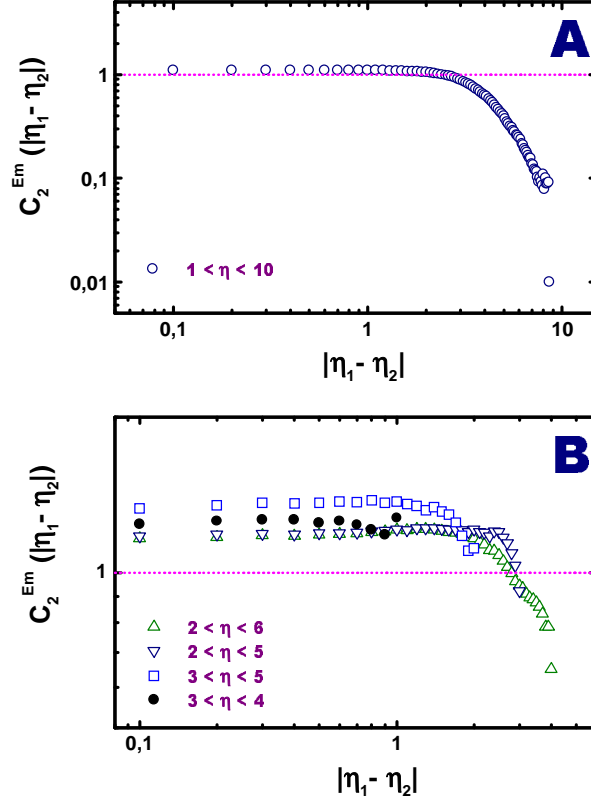


Figure 4: The dependencies of $C_2^{Em}(|\eta_1 - \eta_2|)$ on the η differences $|\eta_1 - \eta_2|$ are drawn in A. C_2^{Em} have values greater than 1 for the η differences < 2.0 . After that their values decrease exponentially. The same relations are drawn in B for the other $\Delta\eta$ intervals. The linear dependencies are also still to be noticed here. Also the exponential decrease for $\delta\eta > 2.0$.

show a power-like scaling. Almost the same behavior we observed in Fig. 1. It is clear that $\delta\eta = |\eta_1 - \eta_2|$ used here does not directly coincident with the bin size $\delta\eta = \Delta\eta/M$ used in Fig. 1 and 2. This linear decreasing with increasing $\delta\eta$ obviously characterizes the expected scaling rule. Therefore, it can be compared with that of the FM (Eq. (7)). As given before the intermittence slopes ϕ_q can be directly retrieved from such log-log scale. If we continue to increase $\delta\eta$, the decrease of C_2^{Em} becomes exponential. And TPCF become smaller than unity.³ For very large $\delta\eta$ some kind of plateau (saturated regions) are formed. In Fig. 3 we showed that TPCF or BEC are applicable only for Q up to ~ 50 MeV/c.

³ The ratios between the correlated and the non-correlated particle-pairs define the two-particle correlation functions C_2 . For the value $C_2 < 1$ we can suppose that the ratios and the corresponding functions are not valid any more.

Figure 4A can be used to visualize the conclusion that the functions $C_2^{Em}(\delta\eta)$ can be compared with $C_2^{Em}(\Delta Q)$. We can therefore conclude that the functions $C(\delta\eta)$ are to be used for $\delta\eta < 2.0$ and eventually, for $\Delta Q < 50$ MeV/c. That the functions $C_2(\delta\eta)$ have linear dependence on the $\delta\eta$ differences until $\delta\eta \approx 2.0$ leads to the assumption that until this value we can describe their dependencies by using a power-law scaling. Then the two values $\delta\eta \approx 2.0$ and $\Delta Q \approx 50$ MeV/c are coincident with each other. They apparently represent the upper limit to consider the TPCF effects. Beyond these values TPCF do not affect the observed FM.

The bottom picture (Fig. 3B) depicts the same relations with the same step-width 0.1 but for the other $\Delta\eta$ intervals. The linear dependencies depending on the $\Delta\eta$ intervals⁴ are also still to be noticed here. They expand also until the value $\delta\eta \approx 2.0$. Although, $C_2^{Em}(\delta\eta)$ for the small $\Delta\eta$ intervals leave the linear dependence earlier than for the large ones evidently, almost the same behavior is also noticed here. There is an interesting finding that the increasing of $\delta\eta$ differences results a giant decreasing of the correlation function $C_2^{Em}(\delta\eta)$. In this regard we can conclude that the effects of TPCF exponentially weakened with increasing the differences $\delta\eta$. Especially, within the two large intervals $2 < \eta < 5$ and $2 < \eta < 6$ we have similar saturated regions as in the top picture. So far we can summarize that the comparison between this figure and Fig. 1 and 2 shows that our investigation of TPCF in dependence on $\delta\eta$ differences results essential information about their contributions to the intermittent behavior.

4.2.4 Strip integral correlations

Using the strip integral correlations given in Section 3 we can calculate FM in dependence on the invariant relative momentum Q . This represents an extension of the second alternative method suggested in Section 4.2.3 to check whether the behavior of TPCF for the orders $q = \{2, 3, 4, 5, 6, 7\}$ can be given by scaling rules similar to that of FM. The results of strip integral correlations are given in Fig. 4.2.4A for the interval $2 < \eta < 6$. Starting with a certain momentum difference we compare it with the calculated relative momentum $|p_1 - p_2|$ by means of the *Heaviside* unit step function \mathcal{H} as given in Eq. (13). We can clearly realize that the increasing of the momentum differences, i.e. increasing the distances between the particles, within which we are searching for the possible particle-pairs which fulfill the condition $Q^2 - (|p_1 - p_2|^2) > 0$ results an additional decreasing of FM. Taking into account the effects of the inner product in Eq. (13) the proportional increasing of FM according to the orders q can be understood.

In light of the scaling Eq. (15) we study the dependence of $C_q^{Em}(\Delta Q)$ on ΔQ for relative momenta ranging from 0.5 until 100 MeV/c. Obviously, we notice that the ability of Eq. (15) to describe these results is limited. Therefore, it should be modified to simulate these *non-linear* relations. The validity of Eq.

⁴ This generally valid for all $\Delta\eta$ intervals. For the first two large intervals as well as for the interval $1 < \eta < 10$, evidently this value is included. For the other two intervals it is excluded, since the differences $|\eta_1 - \eta_2|$ are not enough to reach this value.

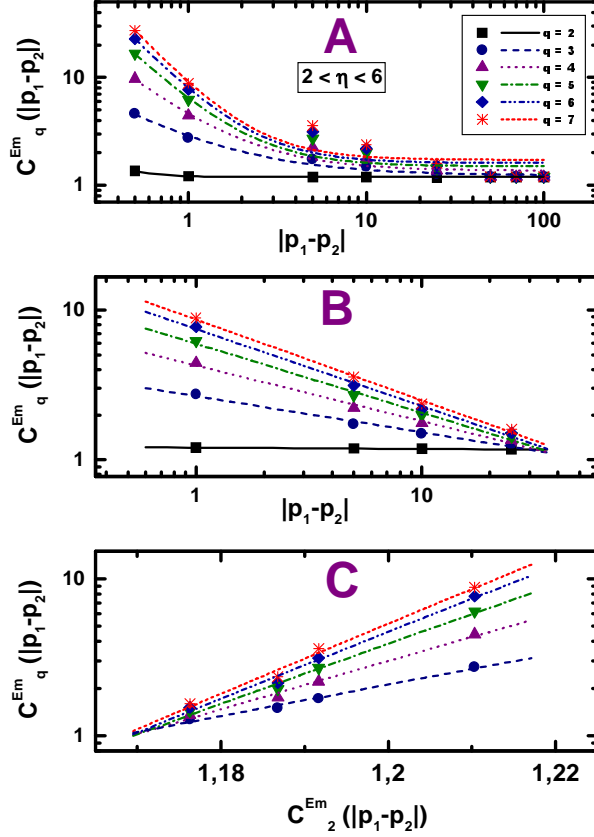


Figure 5: For the orders $q = \{2, 3, 4, 5, 6, 7\}$ the strip density integrals C_2^{Em} are drawn in A as functions of the distances $|p_1 - p_2|$. The experimental results are fitted by using scaling rule given by Eq. (17). The fitting parameters are given in Table 1. The same relations are depicted in B for the region $1 \leq |p_1 - p_2| < 50$ MeV/c. These can good be fitted as straight lines (Eq. (15)). Their fitting parameters are listed in Table 2. The relations between the q -order C_q^{Em} and the second-order ones are illustrated in C. The results are fitted according to Eq. (18). The fitting parameters are listed in Table 3. Although we also use here a log-log scale, the labels of the abscissa are given.

(15) will be discussed later. We would therefore suggest the following empirical power law

$$C_q^{Em}(\Delta Q) = a + b \cdot (\Delta Q)^{-c}. \quad (17)$$

Using this scaling rule the experimental results in Fig. 4.2.4A are fitted and the resulted parameters given in Table 1. We generally notice that for all relations the fitting parameters increase with increasing the orders q . There is only one

exception for $q = 2$, c is too large meanwhile b is too small. By means of this scaling rule it is not possible to retrieve any information about the contribution of TPCF to the observed FM, since the intermittence slopes are entirely hidden. For this destination we should first divide the region $0.5 < \Delta Q < 100$ MeV/c into sub-intervals possibly with common properties. As discussed before TPCF have a restricted region outside of it they are not applicable. Last figure serves to view these properties. Visually, one can notice for instance for $\Delta Q > 50$ MeV/c the values of $\log C_q^{Em}$ are constant for all q .

Although we could not retrieve more experimental points for the region $\Delta Q < 1$ MeV/c, it is to realize that within this region $C_q^{Em}(\Delta Q)$ exponentially decrease with increasing the ΔQ differences. Although this decrease continues even until $\Delta Q \approx 50$ MeV/c, we can notice that the decrease within the region $1 \leq \Delta Q < 50$ MeV/c is not exponential. We still remember the properties of the functions C_q^{Em} within this restricted region. They are comparable with the factorial moments given in Section 3.2. As we noticed they showed an obvious intermittent behavior. Therefore, the subscript q gives the order of FM. For $\Delta Q > 50$ MeV/c we can assure that $C_q^{Em}(\Delta Q) \approx 1.0$ for all ΔQ , i.e. TPCF have no more effects on the observed particle correlations, if the two-particle relative momenta are greater than 50 MeV/c. These facts are visualized in this figure. We obviously notice that all experimental point are saturated.

To study the behavior within the region $\Delta Q < 1$ the experimental data should be first percolated from the Coulomb repulsion. The Gamov correction factor which is usually used to measure the possible interactions between non-coherently emitted particles, i.e. particles simultaneously emitted with almost the same momenta, is about 10% for $\Delta Q \approx 1$ MeV/c. It decreases exponentially with increasing the relative momenta ΔQ . It has a negligible value for few MeV/c. The experimental results used here are not liberated from these interactions. Therefore, we can exclude this small region while studying the dependence of C_q^{Em} on Q .

Table 1: *The relations between $\log C(\Delta Q)$ and $\log \Delta Q$ drawn in Fig. 4.2.4A for $0.5 \leq \Delta Q < 100$ MeV/c are fitted according to Eq. (17). The fitting parameters a , b , and c are listed here. We notice that all values increase with increasing the orders q .*

q	a	b	c
2	1.188 ± 0.002	0.022 ± 0.006	2.882 ± 0.984
3	1.225 ± 0.066	1.654 ± 0.145	1.004 ± 0.116
4	1.365 ± 0.136	3.263 ± 0.339	1.335 ± 0.144
5	1.496 ± 0.211	4.938 ± 0.546	1.607 ± 0.156
6	1.606 ± 0.277	6.405 ± 0.723	1.721 ± 0.161
7	1.721 ± 0.349	7.412 ± 0.913	1.792 ± 0.175

Thence, we are left with the region $1 \leq \Delta Q < 50$ MeV/c, only. For this region the dependence of $C_q^{Em}(|p_1 - p_2|)$ on the relative momenta $\Delta Q = |p_1 - p_2|$ are drawn in Fig. 4.2.4B. We notice that the relations in this log-log scale can

Table 2: Within the region $1 \leq \Delta Q < 50$ the relations $\log C(\Delta Q)$ vs. $\log \Delta Q$ depicted in Fig. 4.2.4B can good be fitted by Eq. (15). We notice that the intermittence slopes ϕ_q increase with the increasing orders q . The constants k represent the intersects.

q	k	ϕ_q
2	$0,083 \pm 0,001$	$0,009 \pm 0,001$
3	$0,426 \pm 0,018$	$0,241 \pm 0,020$
4	$0,631 \pm 0,024$	$0,372 \pm 0,026$
5	$0,776 \pm 0,026$	$0,461 \pm 0,026$
6	$0,874 \pm 0,026$	$0,514 \pm 0,028$
7	$0,937 \pm 0,020$	$0,539 \pm 0,022$

good be fitted as straight lines (Eq. (15)). This behavior is entirely comparable with all pictures in Fig. 1 and in the linear regions in Fig. 4. As given before the tendencies represent the *intermittence slopes* ϕ_q which are listed in Table 2. The increasing the orders q the increasing the slopes ϕ_q . This behavior characterizes the intermittent interacting system. Within this region we can then quantitatively estimate the contributions of TPCF (BEC) to the corresponding FM. To do this we should first study the dependence of the ratios ϕ_q/ϕ_2 on the orders q . Motivated by the Ochs–Wosiek log–log scaling [34] by the adoption of C_q^{Em} to the conventional FM given in Section 3.2 and by the limited validity of Eq. (15) we would therefore recommend the following power-law scaling to be applied within the region $1 \leq \Delta Q < 50$ MeV/c

$$\log C_q^{Em}(\Delta Q) = \frac{\phi_q}{\phi_2} \cdot \log C_2^{Em}(\Delta Q) + k. \quad (18)$$

Table 3: The dependencies of q -order $C_q^{Em}(\Delta Q)$ on the second-order ones depicted in Fig. 4.2.4C for the restricted region $1 \leq \Delta Q < 50$ MeV/c are fitted according to Eq. (15). We clearly notice that the ratios $r_q \equiv \phi_q/\phi_2$ increase with increasing the orders q . Defining the variables $m_q = r_q - \binom{q}{2}$ and $n_q = r_q - (q-1)$ we compared them with r_q . Also the differences between the successive orders of m and n are given.

q	r_q	$-k$	m_q	$m_q - m_{q-1}$	n_q	$n_q - n_{q-1}$
3	$27,52 \pm 2,18$	$1,85 \pm 0,17$	24	23	25	24
4	$42,37 \pm 2,99$	$2,88 \pm 0,22$	36	12	39	14
5	$52,43 \pm 3,63$	$3,56 \pm 0,27$	42	6	48	9
6	$58,43 \pm 4,03$	$3,96 \pm 0,30$	43	1	53	5
7	$61,17 \pm 4,33$	$4,13 \pm 0,33$	40		55	2

The relations between the q -order $C_q^{Em}(\Delta Q)$ and the second-order ones are given in Fig. 4.2.4C. As expected all these log-log relations have positive linear dependencies where the ratios of intermittence slopes ϕ_q/ϕ_2 can directly be retrieved from these relations. ϕ_q/ϕ_2 provide important information about the reaction dynamics and also about the properties of intermittent behavior [21, 23, 31]. The fitting parameters according to the scaling rule Eq. (18) are listed in Table 3. We notice that ϕ_q/ϕ_2 apparently increase with increasing the orders q . These ratios are too large in comparison with $\binom{q}{2}$ which are related to the *self-similar process*. They are also larger than the values resulting from the scaling rule of critical phenomenon characterized by $(q-1)$. For the same data sample we could proof on the one hand that the intermittence slopes ϕ_q/ϕ_2 cannot be simulated as *self-similar process* [23, 31]. Their values are smaller than $\binom{q}{2}$. On the other hand we could partially fit the experimental results according to the critical phenomenon $(q-1)$. In light of these results we try in next section to give an answer to the question “How much can TPCF contribute to the observed FM?”. We will measure their contributions to the most important parameter of the intermittent behavior, namely, the ratios ϕ_q/ϕ_2 .

4.2.5 TPCF contributions to FM

We define $r_q \equiv \phi_q/\phi_2$, $m_q = r_q - \binom{q}{2}$, and $n_q = r_q - (q-1)$. The differences between the successive orders of m and n are also calculated and listed in Table 3. Taking into account the assumption that the contributions of TPCF are linearly added to the observed FM. Furthermore, we know that the experimental values of $\phi_q/\phi_2|_{\text{exp}}$ obtained from FM are calculated over wide ranges of pseudo-rapidity phase-space $\Delta\eta$ (Section 4.1). Then we can suggest to extrapolate them into the relatively small restricted region of the valid TPCF ($\delta\eta < 2.0$ or $\Delta Q < 50$ MeV/c). Therefore, we can suppose that the values of $\phi_q/\phi_2|_{\text{exp}}$ are still valid within the region $1 \leq \Delta Q < 50$ MeV/c. In the language of pseudo-rapidity we suppose the validity of $\phi_q/\phi_2|_{\text{exp}}$ for $\delta\eta < 2.0$. As given above both $\binom{q}{2}$, and $(q-1)$ could be used on the one hand to simulated the experimental results of FM ($\phi_q/\phi_2|_{\text{exp}}$). On the other hand both of them are unable to fit the results of r_q . We noticed from Table 3 that r_q are larger than both $\binom{q}{2}$ and $(q-1)$. According to these assumptions we can suppose to subtract $\phi_q/\phi_2|_{\text{exp}}$ from r_q observed within the region of effective TPCF. Such a way we get a primitive estimation of TPCF contributions to FM. The increasing the orders q the increasing both m_q and n_q . For $\binom{q}{2}$ and $(q-1)$ we can realize that the differences between the successive orders increase with increasing the orders q . In contrast we notice for r_q and correspondingly for both m_q and n_q that the differences of their successive orders decrease with increasing q . For large orders we expect that $m_q = m_{q-1}$ and $n_q = n_{q-1}$. This can be referred to the limited rapidity values of the used data sample and to the restricted available dimension of the emission source.

5 Summary and Final Conclusions

In this article we have studied the non-statistical fluctuations in Pb+Pb collisions at 158 AGeV. First, we would like to sum up the results obtained so far. The analysis of FM in one-dimension shows that the interacting system is obviously intermittent. The phase-space partitions are performed as long as FM increase. For large partition number the increase of FM is exponentially binding upwards. Part of this fast increasing can be understood as TPCF effects. For large $\Delta\eta$ intervals (wide data sample), saturated regions are formed. By continuous increasing the partition number FM continue to rise fast. The difficulties to apply BEC in the emulsion data are shortly discussed. Nevertheless we applied one of the methods suggested in [14]. Using a special analytical expression for TPCF we could retrieve estimations for the dimension of emission source R and for the chaos parameter λ . As expected the randomization parameter $\lambda \approx 1$. This values is an evidence for partially non-coherent emission source and for the simultaneously emitted particles. For the dimension R the value we get is comparable with the r.m.s. ^{82}Pb radius. These results further the use of our method to estimate BEC in the emulsion data sample. This enabled us to directly pass to the main destination of this article. The study of the TPCF contribution to the observed FM. First we studied the dependence of TPCF on the phase-space of pseudo-rapidity (on the differences, $\delta\eta$). For small $\delta\eta$ differences we get linear dependencies for all $\Delta\eta$ intervals until $\delta\eta \approx 2.0$. After that the dependence becomes exponential. This limitation is coincident with the results shown in Fig. 3. An important finding found here is that the boundary between the regions of effective and non-effective TPCF is located around $\delta\eta \approx 2.0$. For relative momenta the boundary is located around $\Delta Q \approx 50$ MeV/c. Defining the region of effective TPCF in $\delta\eta$ enabled us to directly study their intermittent behavior. Using the strip integral correlations we have driven a relation for the TPCF dependence on the phase-space pseudo-rapidity $\delta\eta$ in regard to the intermittent behavior. The dependence of $\log C_q^{Em}(\Delta Q)$ on $\log \Delta Q$ for the region $1 \leq \Delta Q < 50$ MeV/c supports our conclusion that TPCF show an intermittent behavior and probably add considerable values to the conventional FM. The dependence of the intermittence slopes ϕ_q on the orders q can confirm the conclusion concerning the intermittent behavior. To quantitatively estimate the contributions of TPCF we first studied the dependence of q -order C_q^{Em} on the second-order one. Here we noticed that the characterized behavior of intermittency, namely the ratios of intermittence slopes ϕ_q/ϕ_2 increase with increasing the orders q . These ratios are compared with results given in [23, 31]. It is found that on the one hand the values supposed to be added by TPCF increase with increasing the orders. On the other hand the differences between their successive values decrease with increasing orders.

Acknowledgements

I am very grateful to E. Stenlund and all colleagues of EMU01 Collaboration for the helpful discussions and the kind assistance. Especially, that they allowed the use of part of our collaborative experimental data for this work. I would like to thank E. Ganssauge for the continuous support, the interesting discussions, and the helpful comments. It is my pleasure to thank to C. Radke for the careful reading of the manuscript.

References

- [1] R. Hanbury-Brown, R. Twiss, *Phil. Mag.* **54** (1954) 633; *Nature* **178** (1956) 1046; *Nature* **178** (1956) 1447.
- [2] G. Goldhaber, S. Goldhaber, W. Lee, A. Pais, *Phys. Rev.* **120** (1960) 300.
- [3] E. Shuryak, *Phys. Lett.* **B44** (1973) 387; G. Cocconi, *Phys. Lett.* **B49** (1974) 459.
- [4] M. Gyulassy, S.K. Kaufmann, W. Wilson, *Phys. Rev.* **C66** (1979) 2267.
- [5] R. Salmeron, *Winter School on Quark-Gluon Plasma*, Puri, Oressa, India, October 5–16, 1989.
- [6] E.O. Alt, T. Csörgő, B. Lörstad, J. Schmidt-Sørensen, *Eur. Phys. J.* **C13** (2000) 663.
- [7] Review of Particle Physics, *Phys. Rev.* **D54** (1996) 65.
- [8] J. Bjorken, *Phys. Rev.* **D27** (1983) 140; M. Gyulassy, T. Matsui, *Phys. Rev.* **D29** (1984) 419.
- [9] G. Bertsch, *Phys. Rev.* **C37** (1988) 1896.
- [10] S. Pratt, *Phys. Rev. Lett.* **53** (1984) 1219.
- [11] S. Koonin, *Phys. Lett.* **B70** (1977) 43.
- [12] I. Andreev, M. Plümer, R. Weiner, *Phys. Rev. Lett.* **67** (1991) 3475; *Int. J. Mod. Phys.* **A8** (1993) 4577.
- [13] A. Białas, R. Peschenski, *Nucl. Phys.* **B273** (1986) 703; **B308** (1988) 857.
- [14] A.M. Tawfik, to appear in *Acta Phys. Slov.*
- [15] P. Curruthers, E. Friedlander, C. Shih, R. Weiner, *Phys. Lett.* **222** (1989) 487; A. Capella, K. Fiałkowski, A. Krzywicky, *Phys. Lett.* **B230** (1989) 149.

- [16] M. Biyajima, *Prog. Theor. Phys.* **66** (1981) 1378; M. Gyulassy, S. Kaufmann, L. Wilson, *Phys. Rev.* **C20** (1979) 2267; D. Seibert, *Phys. Rev. Lett.* **63** (1989) 136; A. Capella, K. Fiałkowski, A. Krzywicki, *Phys. Lett.* **230** (1989) 149; I. Derado, G. Jancso, N. Schmitz, *Z. Phys.* **C56** (1992) 553; Yu.M. Sinyukov, B. Lörstad, *Z. Phys.* **C61** (1994) 587; T. Wibig, *Phys. Rev.* **D53** (1996) 3586.
- [17] UA1 Collaboration, N. Neumeister et al., *Z. Phys.* **C60** (1993) 633.
- [18] E. Ganssauge, A.M. Tawfik, *Nucl. Instr. Meth.* **A416** (1998) 136.
- [19] A.M. Tawfik, E.Ganssauge, *Comput. Phys. Commun.* **118** (1999) 49.
- [20] EMU01 Collaboration, M.I. Adamovich et al., *Phys. Lett.* **B390** (1997) 445.
- [21] A.M. Tawfik, *Kritische Studien zu der Teilchenkorrelation und den Signaturen des Phasenübergangs in zentralen Blei-Blei-Stößen bei 158 GeV pro Nukleon*, Tectum-Verlag Marburg, 1999, in German.
- [22] P. Curruthers, E. Friedlander, C. Shih, R. Weiner, *Phys. Lett.* **222** (1989) 487; A. Capella, K. Fiałkowski, A. Krzywicki, *Phys. Lett.* **B230** (1989) 149; M. Biyajima, *Prog. Theor. Phys.* **66** (1981) 1378; M. Gyulassy, S. Kaufmann, L. Wilson, *Phys. Rev.* **C20** (1979) 2267; D. Seibert, *Phys. Rev. Lett.* **63** (1989) 136; I. Derado, G. Jancso, N. Schmitz, *Z. Phys.* **C56** (1992) 553; Yu.M. Sinyukov, B. Lörstad, *Z. Phys.* **C61** (1994) 587; T. Wibig, *Phys. Rev.* **D53** (1996) 3586.
- [23] A.M. Tawfik, E.Ganssauge, *Heavy Ion Phys.* **12** (2000) 53.
- [24] S. Pratt, *Phys. Rev.* **D33** (1986) 72; **D33** 1314 (1986), **C42** (1990) 2646; M. Herrmann, G. Bertsch, *Phys. Rev.* **C51** (1995) 325.
- [25] U. Heinz, Talk at *5th Int. Conf. on Relativistic Aspects of Nuclear Physics*, Rio de Janeiro, Brazil, 27–29 Aug, 1997; S. Nickerson, T. Csörgő, D. Kiang, *Phys. Rev.* **C57** (1998) 3251; D. Miśkowiec, S. Voloshin, SGI Scientific Report 1997, p. 87.
- [26] P. Lipa, B. Buschbeck, *Phys. Lett.* **B223** (1989) 465.
- [27] P. Lipa, P. Curruthers, H. Eggers, *Phys. Lett.* **B285** (1992) 300; *Phys. Rev.* **D48** (1993) 2040; P. Lipa, Workshop on *Fluctuations and Fractal Structure*, Ringberg Castel, Germany, 1991, World Scientific Singapore, 1992; S. Chenkanov, W. Kittel, V. Kuvshinov, *Z. Phys.* **C74** (1997) 517.
- [28] E-802 Collaboration, Y. Akiba et al., *Phys. Rev.* **C56** (1997) 1544.
- [29] P. Grassberger, *Phys. Lett.* **A97** (1983) 227; H. Hentschel, I. Procaccia, *Physica* **D8** (1983) 345.

- [30] I. Andreev, M. Biyajima, I. Dremin, N. Suzuki, *Int. J. Mod. Phys.* **A10** (1995) 3951.
- [31] A.M. Tawfik, to appear in *Phys. Lett.* **B**
- [32] OPAL Collaboration, G. Abbiendi et al., *Eur. Phys. J.* **C16** (2000) 423;
WA98 Collaboration, M.M. Aggarwal et al., hep-ex/0008018.
- [33] D. Poal et al., *Rev. Mod. Phys.* **62** (1990) 553.
- [34] W. Ochs, J. Wosiek, *Phys. Lett.* **214B** (1988) 617.